**ACTS Projects SUNBEAM (Smart Universal Beamforming) Deliverable**
**This work is partially sponsored by the European Commission**

| | |
|---|---|
| **Title:** | D321: System Simulation and Algorithm Evaluation |
| **Document Number:** | AC347/UPC/A32/DS/I/006/b1 |
| **Document Type:** | Report |
| **Workpackage:** | WP3 |
| **Organisations:** | ERA, UPC |
| **Authors:** | C. Antón, D. Brooks, J.R. Fonollosa, X. Mestre, P. Thompson |
| **Circulation List:** | SUNBEAM partners |
| **Date:** | 07 September 1999 |

***Abstract***

*The main objective of this report is to carry out a comparative assessment of various array processing algorithms for the UMTS air interface using a common simulation platform at both link and system level.*

***Keyword list***

*Link level simulation*
*System Level simulation*
*Coverage Efficiency*
*Spectral Efficiency*

Feedback and comments may be directed to:

Dr Duncan Brooks, SUNBEAM Project Co-ordinator
ERA Technology Ltd, Cleeve Road, Leatherhead, Surrey, KT22 7SA
Tel: +44 (0) 1372 367055
Fax: +44 (0) 1372 367087
Email: duncan.brooks@era.co.uk

DISCLAIMER

The work associated with this report has been carried out in accordance with the highest technical standards and the SUNBEAM partners have endeavoured to achieve the degree of accuracy and reliability appropriate to the work in question. However since the partners have no control over the use to which the information contained within the report is to be put by any other party, any other such party shall be deemed to have satisfied itself as to the suitability and reliability of the information in relation to any particular use, purpose or application.

Under no circumstances will any of the partners, their servants, employees or agents accept any liability whatsoever arising out of any error or inaccuracy contained in this report (or any further consolidation, summary, publication or dissemination of the information contained within this report) and/or the connected work and disclaim all liability for any loss, damage, expenses, claims or infringement of third party rights.

# 1 INTRODUCTION

This document describes the series of link and system level simulations carried out in WP3 of the SUNBEAM project to evaluate the performance improvement of adaptive antennas into the current specifications of UTRA. It complements the algorithmic studies and link level simulation results reported in the deliverables "Algorithms for Flexible Multi-Standard Array Processing", Parts 1, 2 and 3 incorporating additional link level simulations of multi-user detection schemes. The interface between link and system level simulations is described and justified and preliminary results on spectral and range efficiency are given for different algorithms and for both up and down links.

It was decided at an early stage into the project that the appropriate procedure to influence standards committees of the benefits adaptive antennas was to use as closely as possible the same evaluation procedures that were employed in the selection of UMTS, i.e. the ones given in [ETSIselect]. Although it was possible to extrapolate most of this procedures to the analysis of the influence of adaptive antennas, a certain number of assumptions had to be adopted within the project related to user modelling in the link-level simulations. Additionally, some difficulties appeared when applying the Actual Value Interface between the link and system level simulator. In order to initiate discussion with the relevant standard committees regarding these issues a contribution was presented to the 3GPP TSG-RAN Meeting #3 held in April 1999 in Tokio [TSGRAN].

# 2 ALGORITHM SPECIFICATION

## *2.1 FDD Mode of UTRA*

Two distinct algorithms were initially tested for both the uplink and downlink of the system: the MDIR and the Multi-sensor Rake receivers in the uplink, and the Phased Array and Beamforming with null-steering transmitters in the downlink. For results and details of their implementation, see [D711p1].

This deliverable completes the previous assessment of single user beamforming algorithms and also provides link level results for the CML semi-blind algorithm presented in [D711p3], which was designed to overcome the auto-interfering effects of WCDMA signals.

## *2.2 TDD Mode of UTRA*

In [D711p2], some link-level simulation results of single user beamforming techniques applied to the TDD mode of UTRA were presented. In addition to these results, this deliverable also provides an assessment of Multi-user detection schemes in the TDD mode.

Multi-user detection (MUD) schemes have been known for more than a decade but have been employed in very few practical implementations so far. Initially only highly complex optimal structures were known. Today, however, MUD is mature from a theoretical standpoint and numerous sub-optimal structures of moderate complexity have been derived. Moreover, array observations can be easily introduced in MUD schemes this leading to the so-called Array Joint Detection (AJD) methods. Out of the two modes of UTRA, TDD is particularly well suited for JD schemes. First, the introduction of a time-slotted CDMA multiple access strategy implies that every user of interest experiences a lower number of co-channel interferers. This reduction in the number of intracell interferers makes those schemes computationally affordable.

There also exist other features in the TDD mode that facilitate the use of JD approaches. The use of short spreading sequences makes things easier since, otherwise, signatures would appear to be varying from symbol to symbol which is inherently more difficult to manage. Finally, using a fixed-spreading scheme is also advisable.

Despite that TDD mode clearly favours the use of JD methods, lower complexity traditional beamforming approaches can be used as well. That is, schemes aiming to cancel out interferers by placing a narrowband beamformer prior to a single-user detector (i.e. a MLSE receiver). Within the scope of this paper, performance vs. computational burden trade-off for both types of algorithms will be addressed.

In the light of the discussions above, the following algorithms were selected for the TDD mode: Joint Detection with Minimum Mean Square Error criterion (JD-MMSE) [Jung] and, Matched Desired Impulse Response Receiver (MDIR) [Pipon, Lagunas]. In the following we draw our attention upon the Joint Detection scheme. Details on the implementation of the MDIR architecture in the TDD mode may be found in [D711p2].

As opposed to the MDIR receiver, where each user is detected separately, in the next scheme intracell users will be jointly detected. Contributions from intracell users to the multidimensional received signal are given by:

$$\mathbf{x}(t) = \sum_{n} \sum_{k=1}^{K_d} \mathbf{h}^{(k)}(t - nT)\, s^{(k)}(n) + \mathbf{n}(t)$$

where $s^{(k)}(n)$ denotes the sequence of symbols transmitted by user *k*. Also, each element of the column vector $\mathbf{h}^k(t)$ represents the global system impulse response for a particular sensor and user *k*, including transmission, reception filters, the physical channel response and the corresponding spreading sequence as well. Parameter $K^d$ equals the number of desired (intracell) users and vector $\mathbf{n}(t)$ contains the noise plus intercell interference present in the scenario. After chip-matched filtering, the received signal is sampled at the chip rate. The arrangement of those samples in a single column vector leads to the following expression

$$\mathbf{x} = \left[\mathbf{x}_1^T, \mathbf{x}_2^T, ..., \mathbf{x}_P^T\right]^T = \left[\left[x_{1,1}, x_{1,1}, ..., x_{NM,1}\right]^T, \left[x_{1,2}, x_{1,2}, ..., x_{NM,2}\right]^T, ..., \left[x_{1,P}, x_{1,P}, ..., x_{NM,P}\right]^T\right]^T$$

where *M* stands for the spreading factor, *P* equals the number of sensors, and *N* is the number of symbols transmitted by each active user. Adopting a more convenient matrix notation vector **x** can be expressed in the following terms:

$$\mathbf{x} = \mathbf{H}\mathbf{s} + \mathbf{n}$$

with the combined data vector

$$\mathbf{s} = \left[\mathbf{s}^{(1)^T}, \mathbf{s}^{(2)^T}, ..., \mathbf{s}^{(K_d)^T}\right]^T = \left[s_1, s_2, ..., s_{K_d N}\right]$$

whose components of can be recovered from $s_j = s_n^{(k)}; \quad j = n + N \cdot (k-1)$. Vector **n** contains the samples of the noise plus intercell interference sequence affecting the received signal. The elements in matrix **H** can be obtained by properly rearranging the taps in the sampled versions of $\mathbf{h}^k(t)$ $k$=1...$K$. The basic concept of this approach is given by the set of equations

$$\hat{\mathbf{s}} = \mathbf{M}\,\mathbf{x}$$

where **s** and **x** were defined previously. The choice of matrix **M** determines the equalizer type: zero-forcing equalizer, matched filter, minimum mean square error, etc. In the sequel, we will restrict to the representation of **M** given by the minimum mean square error block linear equalizer (MMSE-BLE) criterion, that is, the one that minimizes the quadratic form $E\left[\left\|\mathbf{s} - \hat{\mathbf{s}}\right\|^2\right]$ with $\hat{\mathbf{s}}$ being the estimate for **s** (see Fig. 1, right). After some algebra, it can be found that matrix **M** amounts to:

$$\mathbf{M} = \left(\mathbf{H}^H \mathbf{R}_n^{-1} \mathbf{H} + \mathbf{R}_s\right)^{-1} \mathbf{H}^H \mathbf{R}_n^{-1}$$

with $\mathbf{R}_n = E\left[\mathbf{n}\mathbf{n}^H\right]$ and $\mathbf{R}_s = E\left[\mathbf{s}\,\mathbf{s}^H\right]$. Hence, derivation of the multi-user receiver requires knowledge of both the combined channel impulse responses for intracell users and the inverse of the covariance matrix associated to intercell interferers ($\mathbf{R}_n^{-1}$). In practice, they will be estimated from the chip-level defined training sequences in the burst midamble (LS-fitting) along with the received snapshots.

Estimating $\mathbf{R}_n^{-1}$, though, is a rather intensive task: both because of the potentially large number of outer product of snapshots that must be performed in order to obtain the $NMP \times NMP$ matrix $\mathbf{R}_n$ and, also, because of the corresponding matrix inversion. Fortunately, computer simulation results in [D711p2] show that noise plus interference is essentially white in the temporal domain and definitively colored in the angular domain. Hence, an approximate expression for matrix $\mathbf{R}_n$ is given by $\mathbf{R}_n \approx \mathbf{\Phi}_n \otimes \mathbf{I}$. where $\mathbf{\Phi}_n$ is the $P \times P$ spatial correlation matrix, $\mathbf{I}$ stands for the $NM \times NM$ identity matrix accounting for temporal (un)correlation, and symbol $\otimes$ denotes Kronecker product. Further, the inverse of the correlation matrix can be expressed as $\mathbf{R}_n^{-1} \approx \mathbf{\Phi}_n^{-1} \otimes \mathbf{I}$. [Brewer]. Thus, the estimation and inversion of a $NMP \times NMP$ matrix can be replaced by the estimation and inversion of a $P \times P$ matrix plus a single Kronecker product.

Further, a sliding window of $\mathbf{N}_s << \mathbf{N}$ symbols is utilized in practice. By doing so, computational complexity is dramatically cut down since all the aforementioned matrices shrink accordingly. Again, this is at the expense of some degradation in performance. However, as pointed out in [Juntti], degradation is very low as soon as a few symbols are included in the sliding window.

# 3 LINK LEVEL SIMULATION RESULTS

## *3.1 FDD MODE OF UTRA*

The link-level results presented within this deliverable complete the series of simulation results presented in [D711p1] for both uplink and downlink of the FDD mode of UTRA. Until now, simulations had been carried out for only two distinct interfering scenarios (1 or 5 directional interfering users) and the High Bit Rate (HBR) users' spreading factors were always set to a fixed value (SF=8). It was therefore necessary to further investigate the impact of both the number of HBR users and their SF on the actual performance of the beamforming algorithms under test. Since a complete evaluation accounting for all ranges of number of users and Spread Factors would have been excessively burdensome, some simulation simplifications (such as the assumption of perfect power control for all users) had to be made.

Basically all the simulation specifications corresponded to those presented in [D711p1], except for what is listed below:

- Variable number of directional (HBR) users: from 1 to 10. The presence of Low Bit Rate (LBR) users is accounted for with the inclusion of background noise.
- Variable Spreading Factor SF=4...32
- Each user was assumed to generate a single Traffic Channel together with the Pilot Sequence. The Control Channel containing the pilot was power-scaled with a weight depending on the Spreading Factor:

| | |
|---|---|
| SF=4 | $a$ = -9 dB |
| SF=8 | $a$ = -6 dB |
| SF=16 | $a$ = -6 dB |
| SF=32 | $a$ = -6 dB |

- Perfect Power Control (with a 0.25 dB disadjustment) for all HBR users.
- All statistics were averaged within a window of 2 slots.

The uplink algorithms were tested in Vehicular_A-(120 km/h) and Pedestrian_A-(3 km/h) channel models (see [SimSpec] for more details).

Figure 1 and Figure 2 show the raw BER results for a Spreading Factor of 4 and 8 respectively. In Figure 3 we have represented the raw BER results as a function of the number of directional users in the scenario for a spreading factor equal to 4. Finally, Figure 4 and Figure 5 serve as comparison among the distinct array processing techniques.

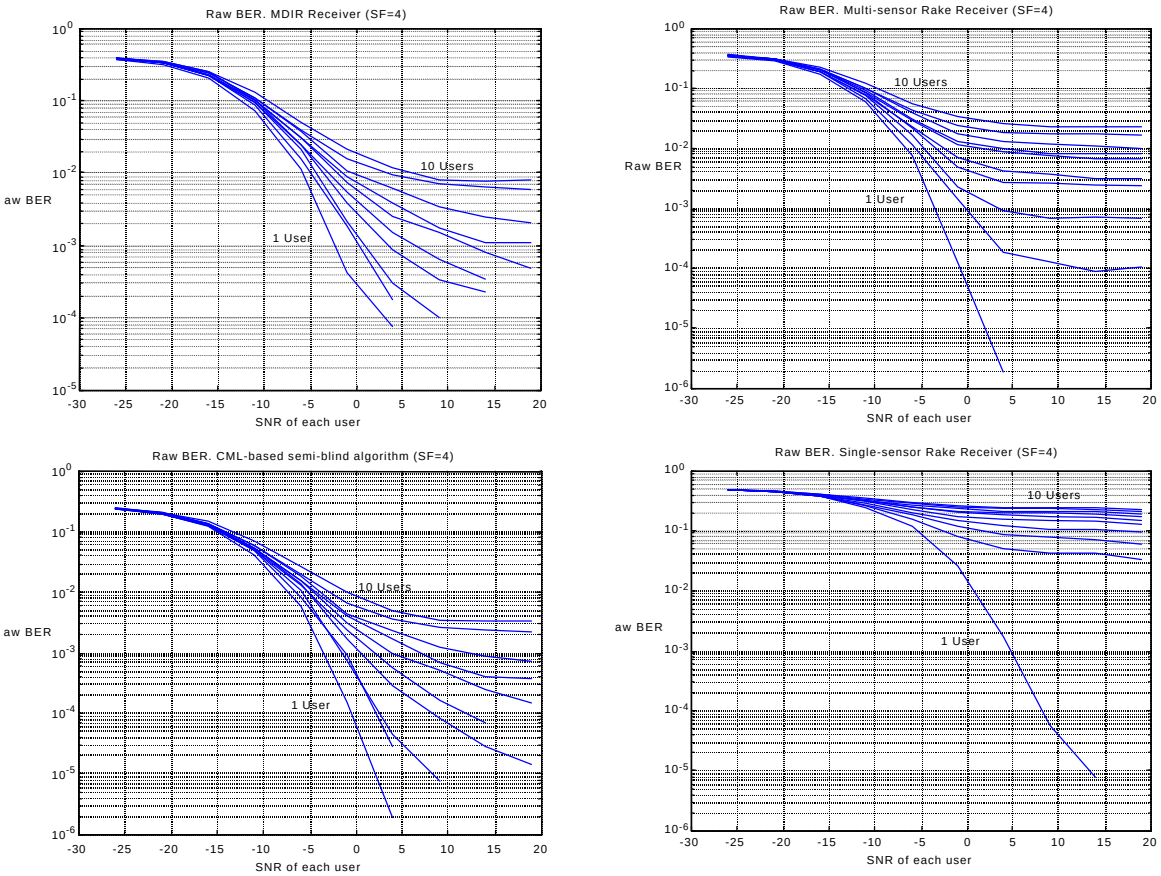


**Figure 1.** Raw BER as a function of the SNR of each user for the Pedestrian channel model with a Spreading Factor of 4. The number of directional users ranged from 1 to 10.

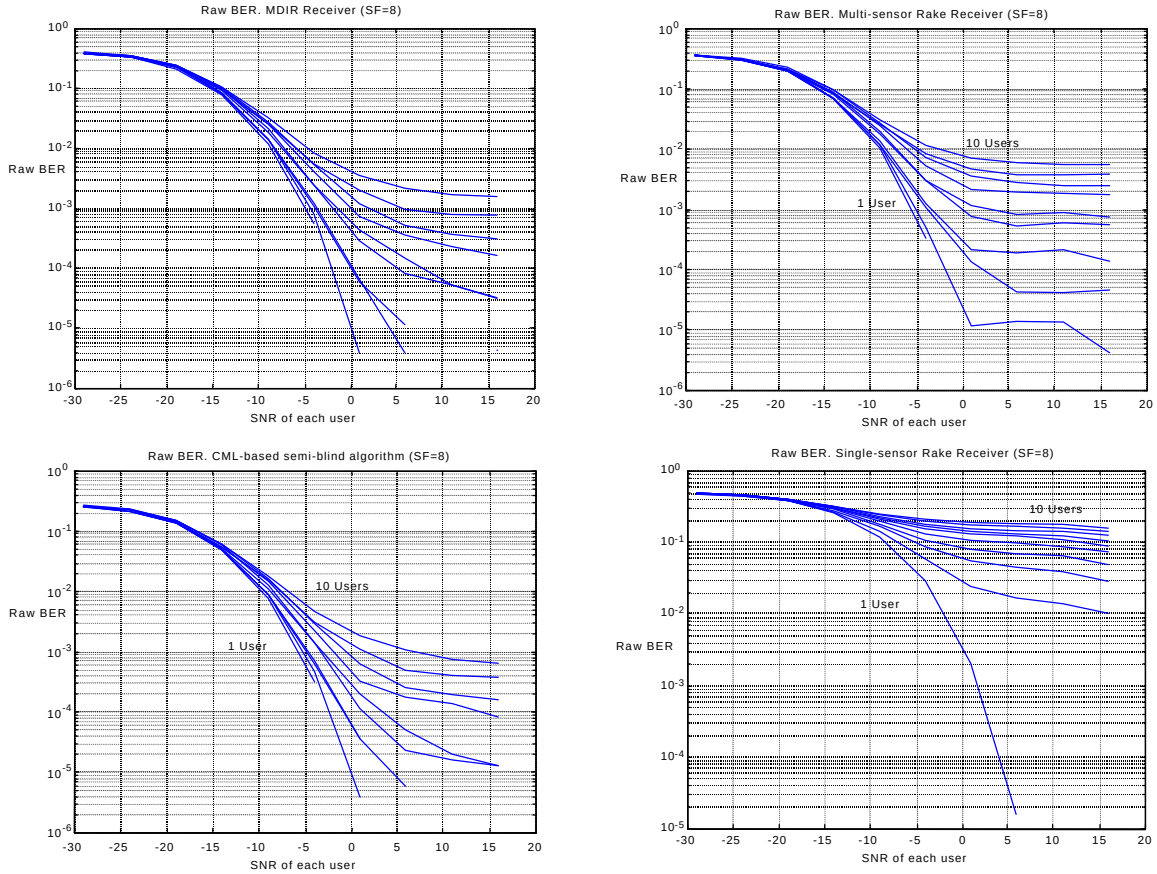


**Figure 2.** Raw BER as a function of the SNR of each user for the Pedestrian channel model with a Spreading Factor of 8. The number of directional users ranged from 1 to 10.

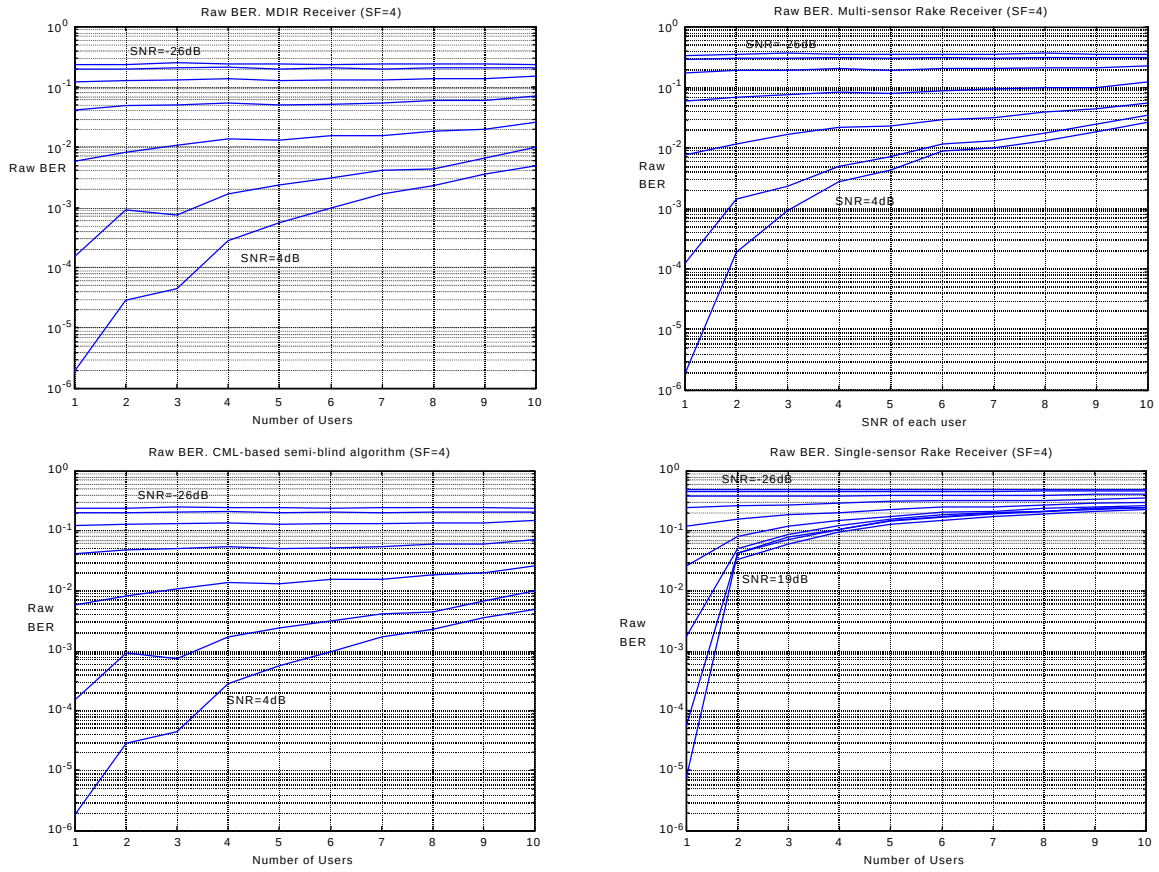


**Figure 3.** Raw BER as a function of the number of directional users for the Pedestrian channel model with a Spreading Factor of 4. The SNR of each user ranged from –26 dB to 4 dB with a step of 5 dB.

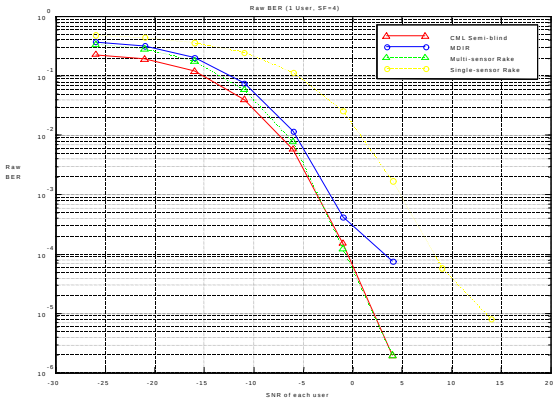


1 Directional User

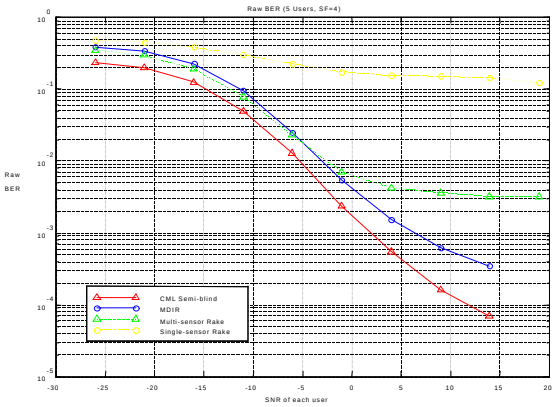


5 Directional Users

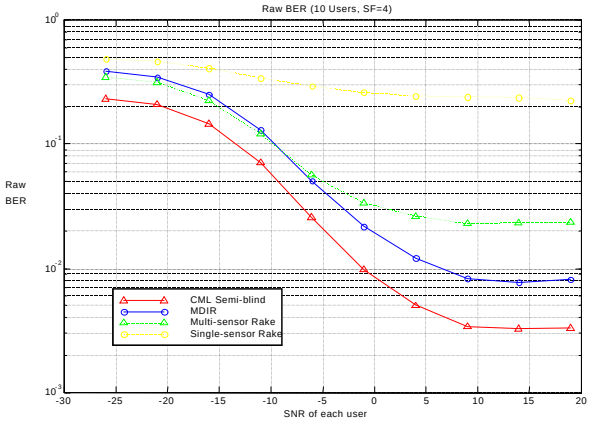


10 Directional Users

**Figure 4.** Raw BER as a function of the SNR of each user for the Pedestrian channel model with a Spreading Factor of 4.

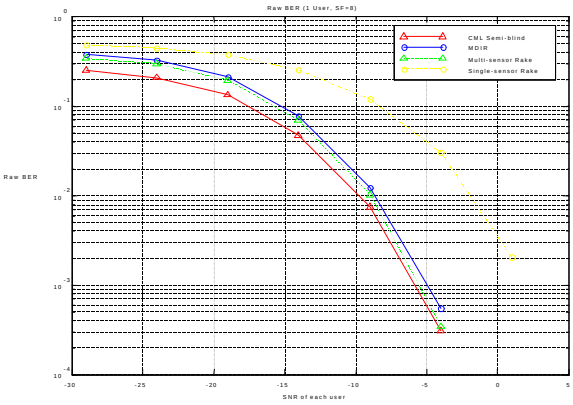


1 Directional User

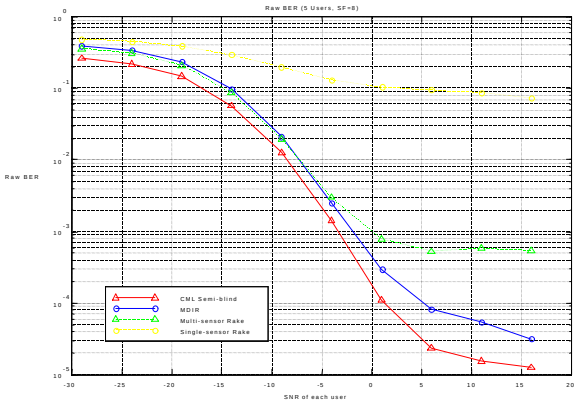


5 Directional Users

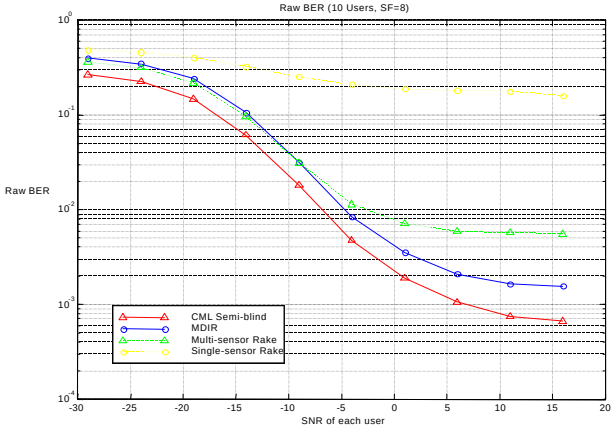


10 Directional Users

**Figure 5.** Raw BER as a function of the SNR of each user for the Pedestrian channel model with a Spreading Factor of 8.

Out of all the proposed techniques, the CML Semi-Blind algorithm proposed in [D711p3] is the one that yields the best results. At the BER region of interest ($10^{-1}$-$10^{-2}$) performances of the Multi-sensor Rake and the MDIR Receivers are very similar, providing gains of more than 5dB with respect to the Single-sensor case.

## *3.2 TDD MODE OF UTRA*

In [ETSI-UTRA], performance of the TDD mode of UTRA in a single sensor case was assessed for the Speech and LCD (Low Constrained Data) services. Accordingly, we will take the same services to evaluate performance enhancement coming from the inclusion of adaptive antennas. However, for brevity, results presented in this report will be restricted to the case where each user (either intracell or intercell) contributes to its timeslot with a single burst, that is, low bit-rate users. Results will always be given in terms of raw (uncoded) BER vs. $E_b/I_o$ curves, where $I_o$ accounts exclusively for intercell interference.

Regarding Vehicular, Pedestrian and Indoor propagation models, both A (mild ISI) and B (severe ISI) subcases were considered in all scenarios, with a probability of occurrence of roughly 50 % each [SimSpec]. However, the width of the sliding window remained constant throughout the whole computer simulation set, such that computational complexity remains moderate. Unfortunately, ISI duration for worst cases falls well beyond window width and, hence, some performance loss can be expected (mostly for the Vehicular channel model) owing to the constant sliding window constrain.

Last, the number of effective intercell interferers was set to 6 for the whole set of computer simulations[1]. Also, and according to the Actual Value Interface (AVI) definition between link- and system-level simulations [Wigard] power control mechanisms were taken into consideration at the link level (further details on these issues can be found in [D711p2]).

For the JD-MMSE algorithm, three versions differing in the way matrix $\mathbf{R}_n^{-1}$ is estimated, were be studied. The lower benchmark for performance is obtained when noise plus interference is assumed to be both temporary and spatially white; thus, making the estimate for $\mathbf{R}_n^{-1}$ to be a diagonal matrix. Hereinafter, this version will be referred to as JD-MMSE-A. Next, when the approximation $\mathbf{R}_n \approx \mathbf{\Phi}_n \otimes \mathbf{I}$ is made (i.e. noise plus interference are assumed temporally white but spatially colored), the algorithm will be called JD-MMSE-B. Last, when the outer product of snapshots is employed to compute $\mathbf{R}_n^{-1}$ (i.e. so assumption is made with respect to its structure) the resulting version will be labeled with JD-MMSE-C.

To begin with, algorithms' performance will be compared for different test channels (Figure 6). Regarding adaptive antenna schemes (left column), higher BERs are experienced for the Vehicular channel. The reason being the combined effects of mobiles' velocity (120 km/h vs. 3 km/h) and, as outlined above, a too short sliding window.

Moving on to the analysis of the JD approaches, JD-MMSE-A constitutes a lower bound for performance in all cases. As soon as interference correlation matrix is more accurately modeled (versions B and C), performance boosts. Trade-off between versions B and C is, unfortunately, difficult to analyze. In the low $E_b/I_o$ region, the computationally intensive version C outperforms version B. However, at a certain point depending on the channel model under consideration, both curves cross each other and algorithms' behaviour changes. This may suggest that, as soon as intercell interference is not that strong and intracell users' channel estimates improve (such estimates must be obtained prior to the computation of $\mathbf{R}_n^{-1}$) version B makes an efficient use of the parametric model embedded in $\mathbf{R}_n^{-1} \approx \mathbf{\Phi}_n^{-1} \otimes \mathbf{I}$. Moreover, performance when estimating $\mathbf{R}_n^{-1}$ in a straightforward manner (outer product of snapshots) may even be worse than that on JD-MMSE-A for high $E_b/I_o$. On the other hand, performance exhibited by the MDIR algorithm is also remarkable. In all scenarios, degradation with respect to JD approaches is actually small whereas complexity is lower.

[1] Since a 120º sectorization scheme is considered, this assumes that 3 intercell users from each neighboring cell are interfering intracell users. The average number of users that are planned to be assigned to each timeslot would approximately be 8; thus, the former assumption on the number of intercell interferers seems to be a rather pessimistic situation.

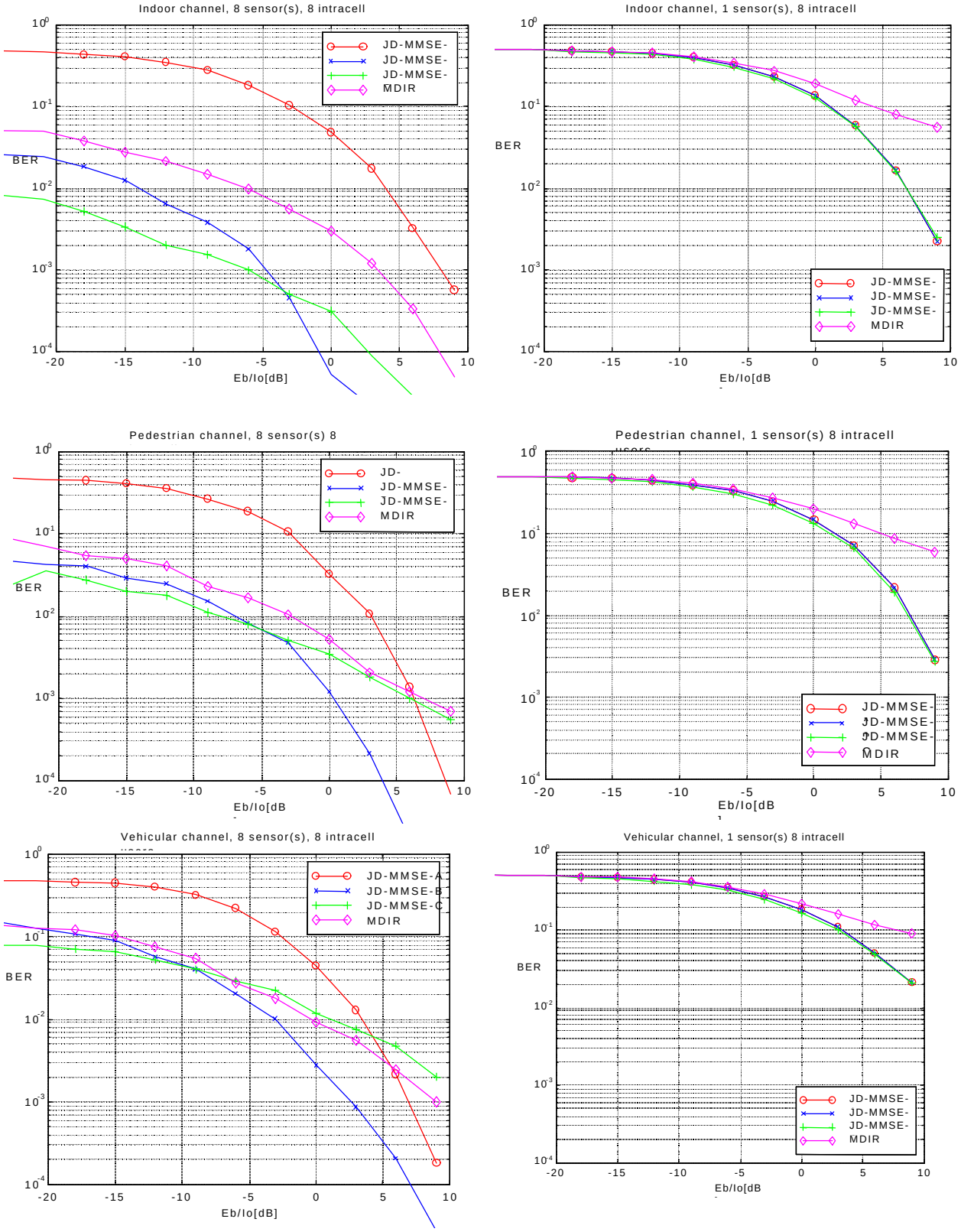


**Figure 6** Uncoded BER vs. Eb/Io for different test environments. Left column: *P*=8 sensors, right column: single sensor. 6 intercell interferers. 8 intracell interferers.

Plots in the right column of Figure 6 (single-sensor case) may help in assessing performance enhancement motivated by the use of array observations. Two comments are due: first, all versions of the JD-MMSE algorithm exhibit almost identical behavior; this strengthens the argument that noise plus interference is predominantly white in the temporal domain. Second, the severe degradation in performance associated to the MDIR curve should also be noted. Actually, this could not be in other way since when MDIR is deprived from multi-sensor observations, it amounts to a channel-matched filter followed by a Viterbi detector. In the presence of colored multiple access interference, this scheme is clearly suboptimal.

Next, Figure 7 depicts BER curves for a number of sensors in the range from 1 to 8 for an Indoor test environment. Since the JD-MMSE-A algorithm assumes intercell interference to be spatially white, it barely exploits the increase in the number of sensors in order to attenuate interference. Actually, improvement is significant when increasing the number of sensors from 1 to 2 but moderate in other cases; this could indicate that this scheme is taking advantage of spatial diversity instead of filtering capabilities only. This is not actually the case for the remaining algorithms or versions, whose performance neatly improves when the number of sensors is increased. For example, in order to yield a target BER of $7 \cdot 10^{-2}$ with the JD-MMSE-B algorithm, an $E_b/I_o$ of 3.0, -3.0 and -13.0 would be necessary when considering 1,2 and 4 sensors respectively.

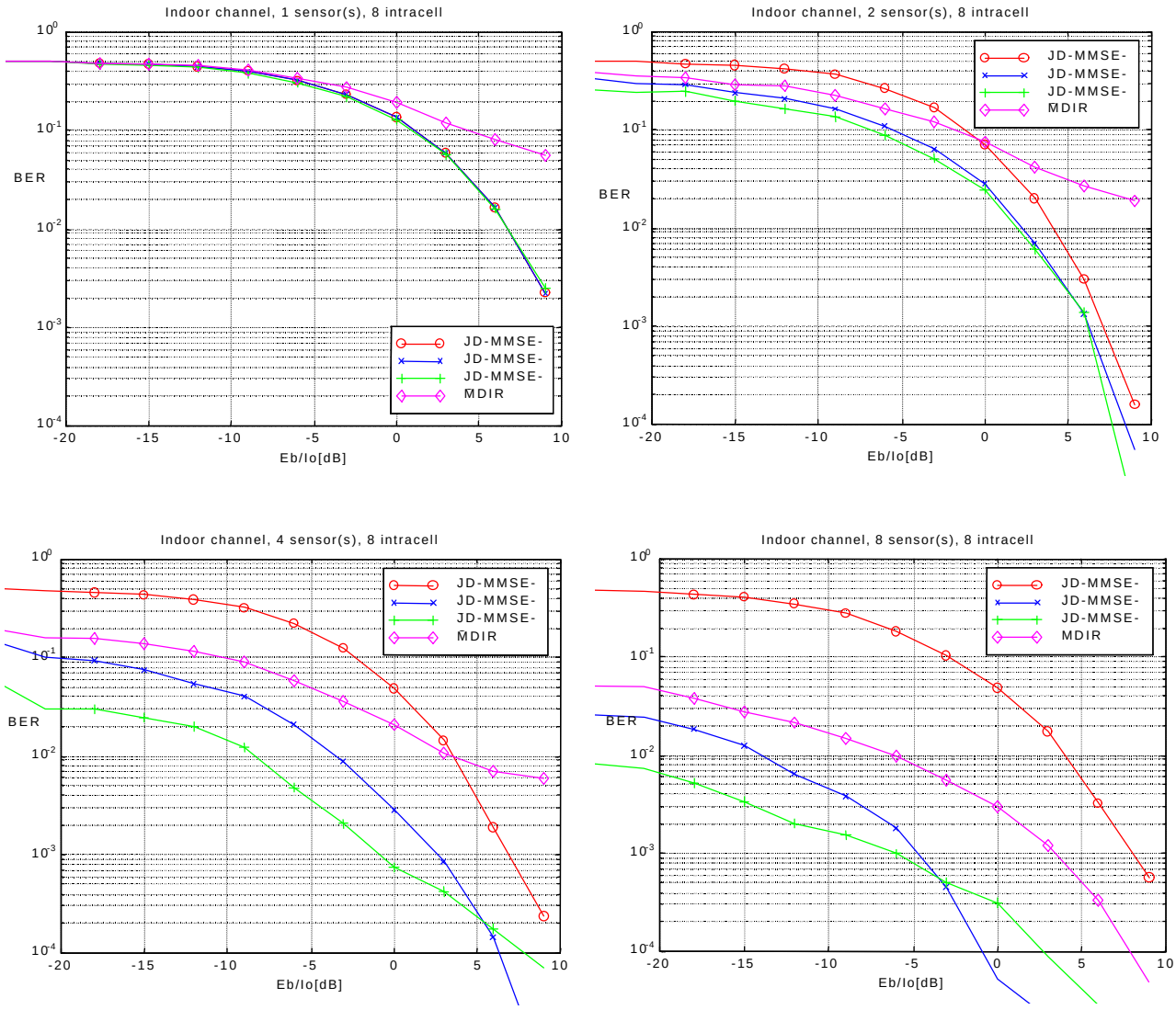


**Figure 7** Uncoded BER vs. Eb/Io for a varying number of sensors with 6 intercell interferers and 8 intracell interferers.

# 4 INTERFACE BETWEEN LINK-LEVEL AND SYSTEM LEVEL SIMULATORS

In order to establish a connection between link and system level simulations, conversion tables between coded and uncoded BER had to be generated. Actual specifications of the channel coding scheme are only established for the FDD mode of UTRA. Thus, the FDD mode was the only mode under consideration.

Basically, four distinct operation modes of the channel coding scheme are defined:

1.- A convolutional encoder, for speech low bit rate services.

2.- A concatenation of a convolutional encoder and a Reed-Solomon code, for high bit rate services.

3.- Turbo codes (under study).

4.- Purpose-built coders (for certain speech services).

Only the first two schemes were considered in our simulations. Table 1 and Table 2 show the configuration of the channel encoder for each type of service under simulation. The Reed-Solomon code was a (255,251) shortened to (36,32) and the convolutional code was either punctured or bit-repeated according to the rate-matching algorithm in [ETSI-UTRA].

| Service | Source Rate (kps) | Physical Channel Rate (kbps) | Info | Coding Time (ms). | Conv. Rate. | Symbol Interleav | Rate Match. | Bit Inteleav. |
|---|---|---|---|---|---|---|---|---|
| Speech1 | 8 | 32 | 80 | 10 | 1/3 | - | 312->320 | 16*20 |
| Speech2 | 8 | 32 | 160 | 20 | 1/3 | - | 552->640 | 20*32 |
| LCD144 | 144 | 512 | 11520 | 80 | 1/3 | 36*20 | 4980->5120 | 16*160 |
| LCD384 | 384 | 1024 | 30720 | 80 | 1/3 | 36*45 | 13272->10240 | 16*320 |
| LCD2048 | 2048 | 1024*6 | 163840 | 80 | 1/3 | 36*640 | 70680->61440 | 16*640 each channel |

**Table 1.** Uplink configuration of the Channel coding scheme for each service under simulation.

| Service | Source Rate (kps) | Physical Channel Rate (kbps) | Info | Coding Time (ms). | Conv. Rate | Symbol Interleav | Rate Match. | Bit Inteleav. |
|---|---|---|---|---|---|---|---|---|
| Speech1 | 8 | 32 | 80 | 10 | 1/3 | - | 312->320 | 16*20 |
| Speech2 | 8 | 32 | 160 | 20 | 1/3 | - | 552->576 | 32*18 |
| LCD144 | 144 | 256 | 11520 | 80 | 1/3 | 36*20 | 326 bits punct. | 128*302 |
| LCD384 | 384 | 1024 | 5120*6 | 80 | 1/3 | 36*45 | 254 bits punct. | 128*814 |
| LCD2048 | 2048 | 1024*4 | 5120*32 | 80 | 1/3 | 36*20 per 1B | 776 bits repet. | 128*4436 |

**Table 2.** Downlink configuration of the Channel coding scheme for each service under simulation.

Figure 8 and Figure 9 present the results for Speech services and Low Constrained Delay services respectively.

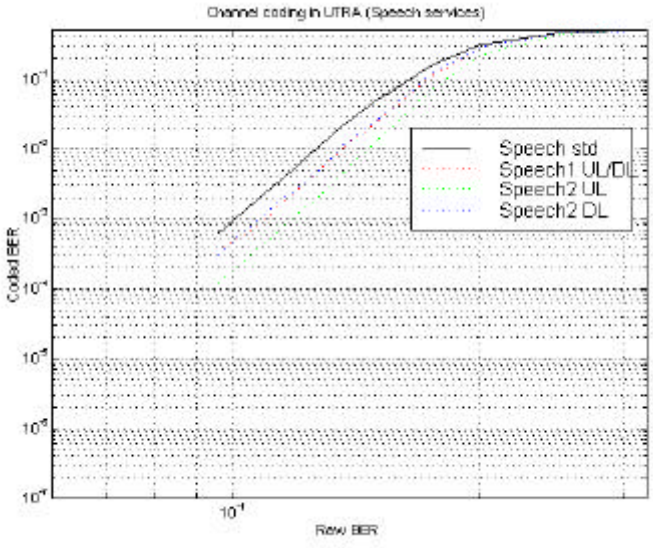


**Figure 8.** Coded BER for Speech Services in UTRA-FDD.

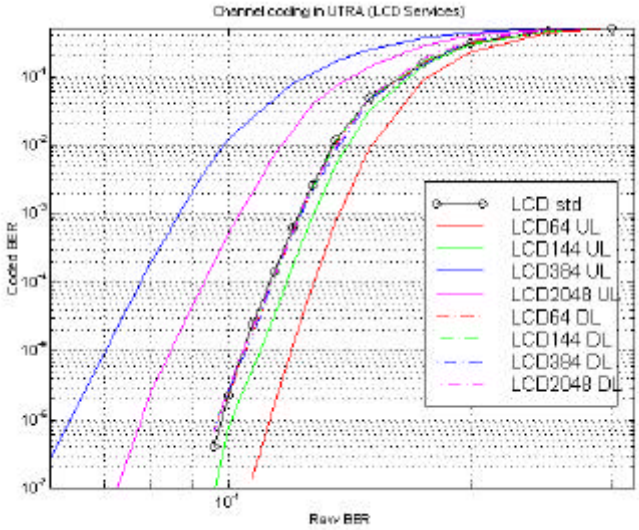


**Figure 9.** Coded BER for Low Constrained Delay Services in UTRA-FDD.

We have also included the curve obtained when no rate-matching procedure is applied (Speech-std, LCD-std). It is observed that when the code is heavily punctured (as in the LCD364UL case), results tend to be rather worse. Conversely, if repetition is used, the BER obtained turns out to be much lower than the standard one, this at the expense of a lower efficiency factor of the convolutional code.

# 5 SYSTEM LEVEL SIMULATION RESULTS

This section presents the results of the system level simulator described in deliverable D311[SimSpec]. Where any enforced differences from the scenarios and methods laid out in that document occur, reference is made in this text to explain the reasoning and possible impact of these minor alterations.

Several points should be held in mind when interpreting these results:

- The handover, power control and channel allocation schemes are very much simplified, but realistic versions of the algorithms which would be deployed in a UTRAN.
- The transmission power and cell sizes are not "concept optimised" [ETSIselect], since it is the algorithms and not the RTT itself which is being tested.
- There is no DOA information in the link/system interface, because the AVI was considered the best existing available for the job.
- Not all scenarios/environments recommended by ETSI [ETSIselect] have been considered, since not all were appropriate or necessary to obtain a sufficiently accurate estimate of algorithm performance.

For these reasons, these results should not be interpreted as an absolute measure of the performance of adaptive antenna algorithms in a UMTS system, but as an indication of the relative performance of the algorithms under test, in relation to each other and the single antenna case. Clearly, much could be done in the way of optimisation of the network parameters for each algorithm which would affect their performance, but this is a vast research topic in its own right and not essential for obtaining the required results to differentiate between the algorithms.

## *5.1 FDD Mode*

### 5.1.1 Uplink

In the FDD mode of UTRA, the uplink and downlink efficiency measures were made separately, as specified by ETSI [ETSIselect], since the frequency bands are separate. The uplink results are presented first, utilising the single sensor Rake, multi-sensor Rake and MDIR algorithms.

Figure 10 shows the effect of increasing the inter-cell distance on the probability that the transmission BER is less than a given threshold ($10^{-3}$ for speech and $10^{-6}$ for LCD data), for the pedestrian (outdoor) and vehicular environments with both speech and LCD144 data. The correspondingly derived values for the coverage efficiency can be seen in Table 3. Figure 11 shows the corresponding effect of increasing cell loading in the same environments and Table 4 contains the resulting spectrum efficiency, calculated when 98% of the users are satisfied.

In the pedestrian environment with speech data, the spatial diversity inherent in the multi-sensor Rake provides a little coverage efficiency improvement over the single-sensor, while

the MDIR gives just under a factor of 2 improvement over the multi-sensor Rake. The low number of users required to test the coverage efficiency can enable the MDIR to achieve sufficiently accurate nulling to make a substantial improvement. In contrast to this, the spectrum efficiency test has so many users per cell that the interference is closer to omnidirectional noise and accurate nulling is not achieved, so the MDIR and multi-sensor Rake give similar performance.

When LCD data is used, the increased interference caused by the low number of users in the coverage tests means that the Rake receivers perform more than a factor of 3 worse with respect to the MDIR, which is able to null out much of this interference. In the spectrum efficiency tests, the low number of high bit rate users required to achieve maximum loading again results in a large performance differential of over 20 times between MDIR and Rake receivers.

In the vehicular environment, the larger delay spreads and rate of fading have a pronounced effect. When speech data is used for the coverage test, the low number of users still enables the MDIR to outperform the Rake receivers by a factor of 2, but in the spectrum tests, a factor of 6 difference is observed. The single sensor Rake is right on the range limit and so no meaningful results were obtained, but the degradation suffered by the multi-sensor Rake is much greater than for the MDIR with respect to the pedestrian environment.

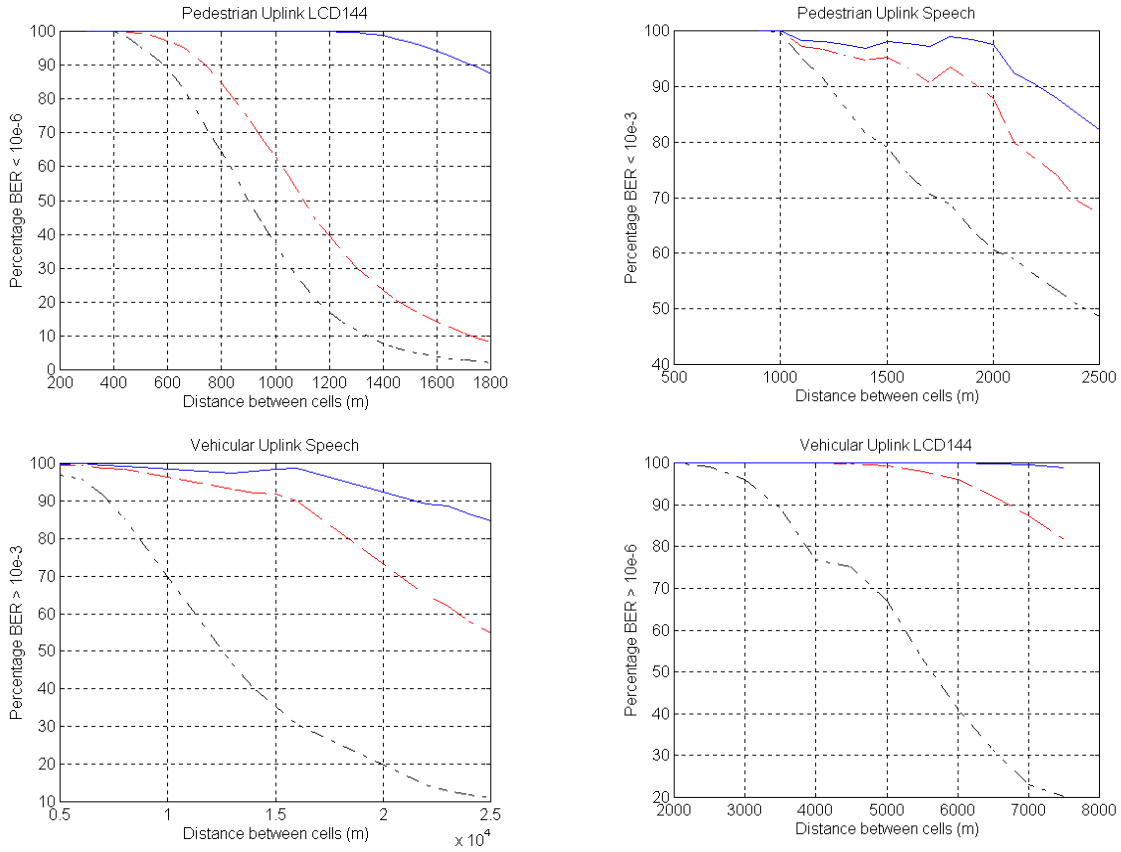


**Figure 10.** Coverage efficiency results for FDD Uplink: MDIR receiver (solid line), Multi-sensor Rake receiver (dashed line) and Single-sensor Rake receiver (dash-dotted line).

| | Pedestrian FDD Uplink | | | | Vehicular FDD Uplink | | | |
|---|---|---|---|---|---|---|---|---|
| | Speech | | LCD144 | | Speech | | LCD144 | |
| Algorithm | Range (m) | Coverage ($km^2$/cell) | Range (m) | Coverage ($km^2$/cell) | Range (m) | Coverage ($km^2$/cell) | Range (m) | Coverage ($km^2$/cell) |
| RAKE | 550 | 0.20 | 250 | 0.04 | 3035 | 5.98 | 1570 | 1.60 |
| VRAKE | 750 | 0.37 | 335 | 0.07 | 5535 | 19.90 | 3070 | 6.12 |
| MDIR | 1025 | 0.68 | 775 | 0.39 | 9020 | 52.85 | 4500 | 13.15 |

**Table 3.** FDD Uplink Coverage efficiency summary

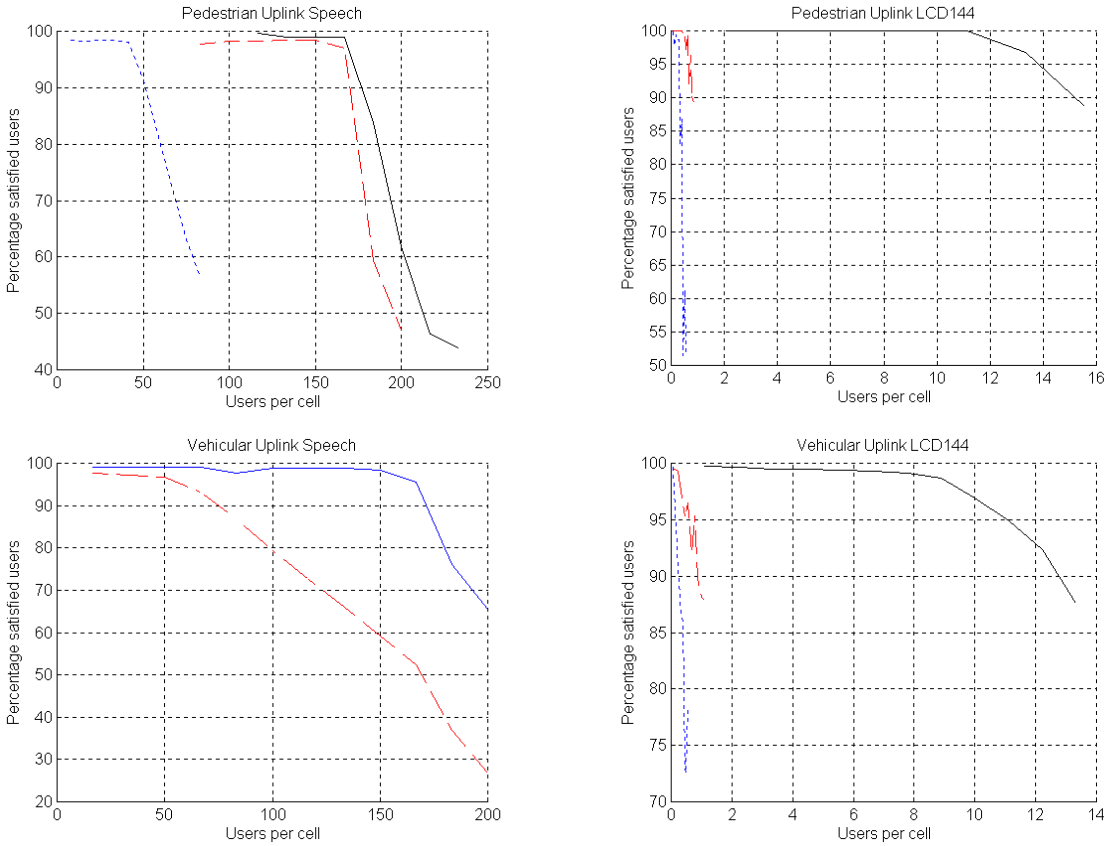


**Figure 11.** Spectrum efficiency results for FDD Uplink: MDIR receiver (solid line), Multi-sensor Rake receiver (dashed line) and Single-sensor Rake receiver (dash-dotted line).

| | Pedestrian FDD Uplink | | | | Vehicular FDD Uplink | | | |
|---|---|---|---|---|---|---|---|---|
| | Speech | | LCD144 | | Speech | | LCD144 | |
| Algorithm | Users/ Cell | Spectrum Efficiency (kbits/s/ MHz/Cell) | Users/ Cell | Spectrum Efficiency (kbits/s/ MHz/Cell) | Users/ Cell | Spectrum Efficiency (kbits/s/ MHz/Cell) | Users/ Cell | Spectrum Efficiency (kbits/s/ MHz/Cell) |
| RAKE | 40 | 32 | 0.3 | 8 | - | - | 0.1 | 2 |
| VRAKE | 158 | 126 | 0.6 | 17 | 27 | 21 | 0.4 | 11 |
| MDIR | 171 | 136 | 12.5 | 360 | 155 | 124 | 9.1 | 262 |

**Table 4.** FDD Uplink spectrum efficiency summary

Once again, in the coverage test for LCD data, the same capability of the MDIR with low numbers of users gives a factor of 2 gain in efficiency. The spectrum results show the same effects in the vehicular environment with LCD data as with speech, except that this time the

differences between MDIR and Rake are compounded by the low number of high bit rate users, giving a factor of 20 difference. It should be noted that as in [ETSI-UTRA], the spectrum test for LCD144 was done using 1.5km cell separation as opposed to 6km suggested in [ETSIselect]. This is because of poor performance giving no meaningful results due to the reduced range.

### 5.1.2 Downlink

In the FDD downlink, Downlink Phased Array (DPA) and Downlink Beamforming with Null Steering (DBNS) are compared with the performance of a single antenna. The performance of these algorithms is shown for the pedestrian and speech environments with speech and LCD data, in terms of coverage and spectrum efficiency respectively, in Figure 12 and Figure 13. Summaries are shown in Table 5 and Table 6.

In the pedestrian environment with speech data, Figure 13 shows the large increase in spectrum efficiency which can be obtained by using directional beamforming. An improvement factor of approximately 4 can be seen over the single antenna case. The large number of users imposes constraints that cannot be met on the DBNS algorithm in terms of the nulling required and hence the performance is slightly degraded with respect to the DPA algorithm. A coverage efficiency increase of up to 80% over the single antenna can also be observed from the results.

When changing to LCD data, the low number of users in the coverage tests means that the accuracy of the nulls created by DBNS is not so important and hence it is able to do better than DPA, giving improvements over single antenna of approximately 5 as compared to 2 for DPA. The spectrum tests involve more users, but still not sufficiently many to degrade the DBNS performance greatly and this gives a performance improvement of approximately 4 for both DBNS and DPA.

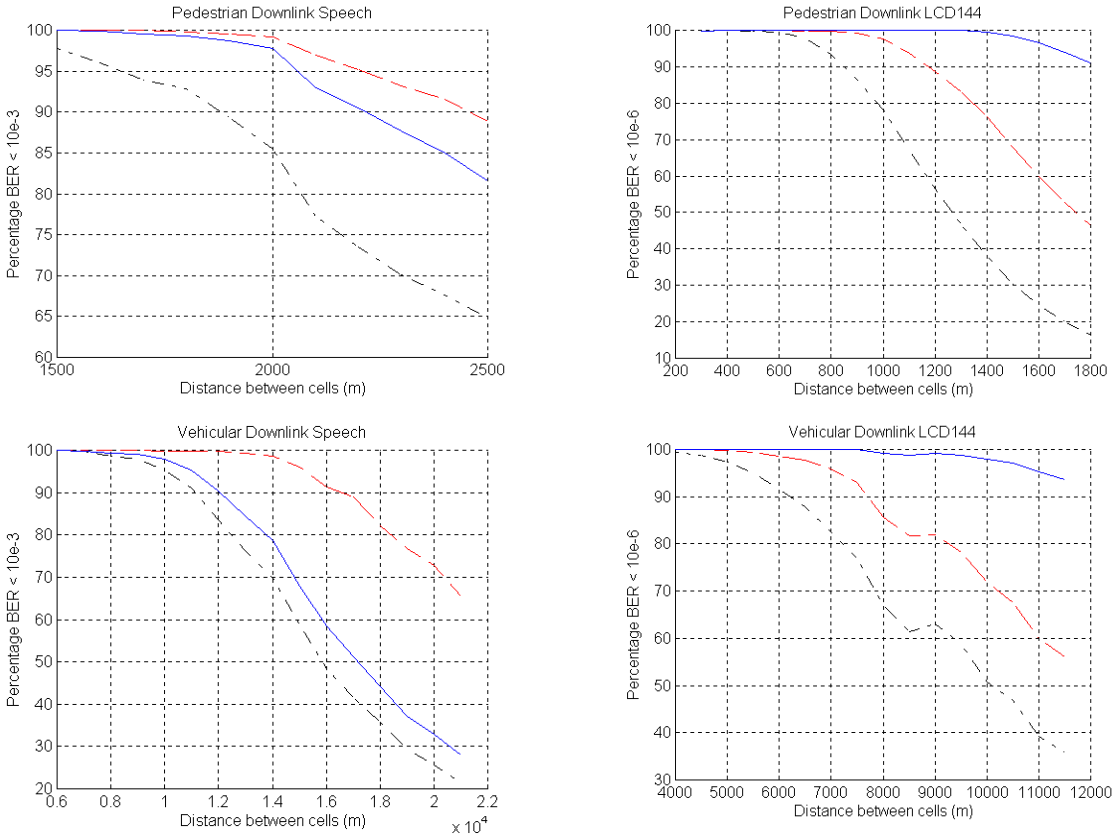


**Figure 12.** Coverage efficiency results for FDD Downlink: DBNS (solid line), DPA (dashed line) and Single-sensor transmitter (dash-dotted line).

| | Pedestrian FDD Downlink | | | | Vehicular FDD Downlink | | | |
|---|---|---|---|---|---|---|---|---|
| | Speech | | LCD144 | | Speech | | LCD144 | |
| Algorithm | Range (m) | Coverage ($km^2$/cell) | Range (m) | Coverage ($km^2$/cell) | Range (m) | Coverage ($km^2$/cell) | Range (m) | Coverage ($km^2$/cell) |
| 1 sensor | 820 | 0.44 | 375 | 0.09 | 5050 | 16.56 | 2780 | 5.02 |
| DPA | 1110 | 0.8 | 540 | 0.19 | 7700 | 38.51 | 3600 | 8.42 |
| DBNS | 1030 | 0.69 | 830 | 0.45 | 5500 | 19.65 | 5580 | 20.22 |

**Table 5.** FDD Downlink Coverage efficiency summary.

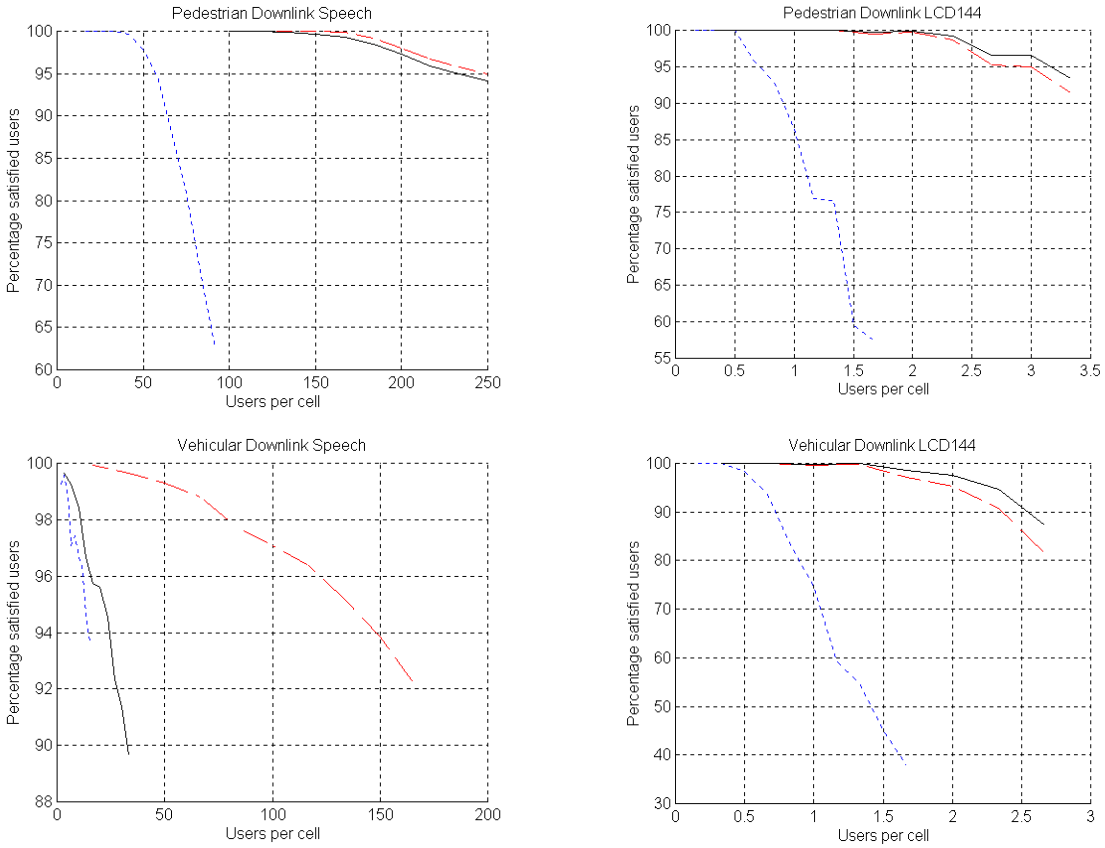


**Figure 13.** Coverage efficiency results for FDD Downlink: DBNS (solid line), DPA (dashed line) and Single-sensor transmitter (dash-dotted line).

| | Pedestrian FDD Downlink | | | | Vehicular FDD Downlink | | | |
|---|---|---|---|---|---|---|---|---|
| | Speech | | LCD144 | | Speech | | LCD144 | |
| Algorithm | Users/ Cell | Spectrum Efficiency (kbits/s/ MHz/Cell) | Users/ Cell | Spectrum Efficiency (kbits/s/ MHz/Cell) | Users/ Cell | Spectrum Efficiency (kbits/s/ MHz/Cell) | Users/ Cell | Spectrum Efficiency (kbits/s/ MHz/Cell) |
| 1 sensor | 48 | 38 | 0.6 | 17 | 7 | 5 | 0.5 | 14 |
| DPA | 200 | 160 | 2.4 | 69 | 79 | 63 | 1.6 | 46 |
| DBNS | 187 | 149 | 2.5 | 72 | 13 | 10 | 2 | 57 |

**Table 6.** FDD Downlink spectrum efficiency summary.

The more taxing vehicular environment provides a stark contrast between DPA and DBNS performance. The increased speed, fading rate and delay spread are crucial in degrading the

spatial signature estimate, resulting in poor nulling accuracy. Almost no improvement in coverage efficiency and only a factor of 2 in spectrum efficiency is achieved by the DBNS over single antenna, where as the DPA achieved factors of 2 and 10 respectively. These tests illustrate the sensitivity of the DBNS to poor spatial data, which does not impact so heavily on the DPA.

The adverse environment does not have such a great effect on the DBNS in the LCD data case, where there are less users to direct nulls towards. Improvement factors over the single antenna of up to approximately 4 in both coverage and spectrum efficiency were achieved. Once again, to enable fair comparison between up and downlink, a 1.5km cell spacing was used in the spectrum tests for LCD144 data.

# 6 CONCLUSIONS

This document has described a series of link and system level simulations carried out in WP3 of the SUNBEAM project to evaluate the performance improvement of adaptive antennas into the current specifications of UTRA. The results have built on the algorithmic studies and link level simulation results reports in the deliverables "Algorithms for Flexible Multi-Standard Array Processing", Parts 1, 2, and 3, by incorporating link and system level simulations of multi-user detection schemes. The interface between link and system level simulations was described and justified and results on spectral and range efficiency were given for uplink and downlink algorithms.

In drawing conclusions from the system level results in this report, it is important to understand the trade-offs which are inherent in the design criteria. On top of the usual issues of performance versus complexity, the flexibility of any algorithms to operate in different environments and even within different Radio Transmission Technology modes is also of importance.

The results presented here provide an overview of the possible performance gains of the various algorithms at the system level and their relative complexity can be deduced from the format of the algorithms given in the link level studies. However, in order to obtain a lower level view of the performance and complexity trade off (as well as the flexibility issues), the DSP implementational work of WP5 should also be considered when forming conclusions about the suitability of the algorithms. This work provides a complementary view on the complexity and link level performance.

It is clearly desirable to design algorithms which will be equally suited to all modes of operation and all environments, but algorithm derivation and simulation results soon make it clear that some will be more suited to different environments and modes. For this reason, the different environments are considered separately, before drawing general conclusions.

For the FDD uplink pedestrian environment, the MDIR gives only marginal performance benefits in terms of the spectrum efficiency, which taken on its own would imply the use of the multi-sensor RAKE algorithm. However, the coverage improvements and performance with LCD data provide sufficient justification for the moderate complexity increases involved. The vehicular environment provides a much clearer comparison, since the MDIR outperforms the multi-sensor RAKE in all services, owing to the severe nature of the radio channel.

The FDD downlink issues are slightly more complex, in that DBNS weights can be obtained directly from the MDIR algorithm (after frequency translation) which saves on complexity. However, the accuracy of calibration and frequency translation schemes for uplink and

dowlink have not been considered in this report since they are separate issues in themselves and are considered in detail in WP6. It is known that these matters impact adversely on the accuracy of nulling and hence overall performance. It is noticeable that, even without calibration errors, the ability of DBNS to position nulls accurately is dubious because of poor correlation matrix estimation on the uplink caused by traffic channel interference and slot averaging effects. It may be that modifications which are currently under investigation will improve the situation, but in its present form, the DPA would appear to be more suited to the downlink than DBNS, particularly in the more challenging vehicular environment.

Since the MDIR can also be used for the TDD mode of UTRA, it possesses a flexibility advantage over the multi-sensor RAKE as well. Even if it were not for this reason, the system level results would indicate that MDIR (or some modification of it) would be suitable for use in the uplink of UTRA base stations. Similarly, with the present algorithms, the FDD downlink would be favoured by the use of DPA.

# 7 REFERENCES

[Brewer] J.W. Brewer, "Kronecker Products and Matrix Calculus in System Theory", IEEE Trans. on Circuits and Systems, Vol. 25, No. 9, pp. 772-781, Sept. 1978.

[D711p1] X. Mestre, C. Antón, J. R. Fonollosa, "Algorithms for Flexible Multi-Standard Array Processing: Part 1, FDD Mode of UTRA", Deliverable D711, AC347/UPC/A71/PI/I/005/b1, ACTS 0347 SUNBEAM project.

[D711p2] C. Antón, X. Mestre, J. R. Fonollosa, "Algorithms for Flexible Multi-Standard Array Processing: Part 2, TDD Mode of UTRA", Deliverable D711, AC347/UPC/A71/PI/I/005/b1, ACTS 0347 SUNBEAM project.

[D711p3] X. Mestre, J. R. Fonollosa, "Algorithms for Flexible Multi-Standard Array Processing: Part 3", Deliverable D711, AC347/UPC/A72/PI/I/007/b1, ACTS 0347 SUNBEAM project.

[Jung] P. Jung and J. Blanz, "Joint detection with coherent receiver antenna diversity in CDMA mobile radio systems", IEEE Trans. on Vehicular Technology, Vol. 44, No. 2, pp. 76-88, Feb. 1995.

[Juntti] M. Juntti, "Multiuser demodulation for DS-CDMA systems in fading channels", Ph.D. Thesis, University of Oulu (Finland), 1997.

[Lagunas] M.A. Lagunas, A. Perez-Neira, J. Vidal, "Optimal Array Combiner for Sequence Detectors", Proceedings of the IEEE International Conference on Acoustics, Speech and Signal Processing ICASSP-98, vol IV, pp. 3341-3344, Seattle, May 12-15, 1998.

[ETSIselect] Technical Report, "Universal Mobile Telecommunications System (UMTS); Selection procedures for the choice of the radio transmission technologies of the UMTS", UMTS 30.03 version 3.2.0, 1998.

[ETSI-UTRA] "Submission of Proposed Radio Transmission Technologies: the ETSI UMTS Terrestrial Radio Access (UTRA) ITU-R RTT Candidate Submission", ETSI SMG2. Date of submission: 29/1/1998. Available at the ITU WWW http://www.itu.ch/imt/

[Pipon] F. P. Pipon, P. Chevalier, P. Villa, J-J Monot, "Joint Spatial and Temporal Equalization for channels with ISI and CCI – Theoretical and Experimental results for a base station reception", Proc. IEEE Signal Processing Workshop on Signal Processing Advances in Wireless Communications, Paris, France, April 1997, pp. 309-312.

[SimSpec] Mestre X., Antón C., Fonollosa J. R., "System Simulation Specification", Deliverable D311, AC347/UPC/A31/PI/I/002/a3, ACTS-SUNBEAM.

[TSGRAN] Antón C., Mestre X, Fonollosa J. R., "Performance Evaluation of Adaptive Antennas in UTRA", Input of the ACTS-SUNBEAM project to the 3th·3GPP

TSG-RAN Meeting, Tdoc 247 Tokio, Japan, April 21-23, 1999, presented by Motorola.

[Wigard] J. Wigard and P.Mogensen, "A Simple Mapping from C/I to FER and BER for a GSM Type of Air-Interface", Proc. of the Personal and Indoor Mobile Radio Conference (PIMRC), Taipei (Taiwan), Sept.1996.